IJES *Iranian Journal of Earth Sciences*
Vol. 11, No. 4, 2019, 256-266.

Detection of metallic prospects using staged factor and fractal analysis in Zouzan region, NE Iran

Hamed Abdoli Sereshgi[1], Alireza Ganji[2*], Afshin Ashja Ardalan[1], Habibollah Torshizian[3], Jafar Taheri[4]

1. Department of Geology, North Tehran Branch, Islamic Azad University, Tehran, Iran
2. Department of Geology, Lahijan Branch, Islamic Azad University, Gilan, Iran
3. Department of Geology, Mashhad Branch, Islamic Azad University, Mashhad, Iran
4. Geological Survey of Iran North-East Territory General Manager, Mashhad, Iran

Received 16 October 2018; accepted 7 May 2019

Abstract

The Zouzan area is located in the SE of Torbat-e- Heydarieh city (NE Iran). This area is located on north part of the Lut block which consists of basaltic andesite, tuff and porphyritic andesite. The purpose of this research is to investigate the enrichment of metal elements in the Zouzan area and provide a metallic geochemical model. For this purpose, 488 stream samples were analyzed using by ICP-MS. The results were interpreted using staged factor analysis to determine the components that are rich in the study area. However, Concentration-Number (C-N) fractal modeling was used for interpretation of these data and presenting a final model. The results of this study indicate the concentration of anomalies of the Au, Ag, Cu, Pb and Zn as main elements in the central, NE and SW of the Zouzan area. Moreover, results obtained by the staged factor analysis shows the elements of the specified components by this method that enriched together in the study area. The place of enrichment is in the central NE and SW parts of the study area.
Keywords: *Zouzan, Geochemical anomalies, Staged factor analysis, Concentration-Number (C-N) fractal modeling*

1. Introduction

The Zouzan area located in North part of the Lut block in East of Iran approximately 80 km SE of the Torbat-e-Heydarieh town (Fig 1). The Lut Block is one of the micro continental blocks which is interpreted to have drifted from the northern margin of Gondwanaland during the Permian opening of the Neo-Tethys, which was subsequently accreted to the Eurasian continent in the Late Triassic during the closure of the Paleo-Tethys (Golonka 2004). The tectonic and magmatic evolution of the Lut block has been interpreted within an extensional setting (Tarkian et al. 1983; Jung et al. 1984). The presence of ophiolitic complexes in Eastern Iran between the Lut and the Afghan blocks, led (Saccani et al. 2010) to consider the subduction of the oceanic lithosphere at this zone, while (Eftekharnejad 1981) proposed that magmatism in the northern Lut area resulted from the subduction of Afghan block beneath the Lut block (Berberian 1983). It is indicated that igneous rocks at Lut block have a calc-alkaline arc signature. The polarity of the accretionary prism-fore arc basin, the structural vergence, and younging of the accretionary prism to the southwest are consistent with a NW-dipping subduction scenario (Tirrul et al. 1983). Recently, asymmetric subduction models have been discussed for situations similar to that of the Lut block (Arjmandzadeh 2011).

---
*Corresponding author.
E-mail address (es): ar_ganji2000@yahoo.com

Doruneh Fault extends some 900 km from the north to the Jazmorian basin in the south and is ~ 200 km wide (Stocklin and Nabavi 1973). The Lut Block consists of a pre-Jurassic metamorphic basement, Jurassic sedimentary rocks and several generations of Late Mesozoic and Cenozoic intrusive and/or volcanic rocks (Camp and Griffis 1982; Tirrul et al. 1983). Radiometric age data indicate that the oldest magmatic activity in the central Lut Block took place in the Jurassic. Rb-Sr isotope data from the whole-rock and the biotite from the Sorkh Kuh granitoid yield Middle to Late Jurassic ages (164.8 ± 1.9 Ma and 170 ± 1.9 Ma respectively; (Tarkian et al. 1983). Intrusive rocks of a similar age are also recognized in the Deh-Salm metamorphic complex in the eastern Lut Block (Mahmoudi et al. 2010). Further to the north, magmatic activity started in Upper Cretaceous (75 Ma) and generated both volcanic and intrusive rocks (Tarkian et al. 1983). The Middle Eocene (47 Ma) was characterized by alkaline and shoshonitic volcanism with a peak at the end of the Eocene. In addition, calc-alkaline basalts and basaltic andesites were erupted in the Eocene-Oligocene (40–31 Ma); (Tarkian et al. 1983; Malekzadeh 2009; Karimpour 2011; Saadat and Stern 2016).

2. Geological setting

The major rock types in the Zouzan area are Cenozoic calc-alkaline volcanic rocks and the spatially and temporally related sub volcanic intrusive stocks are exposed along the NW-SE direction.

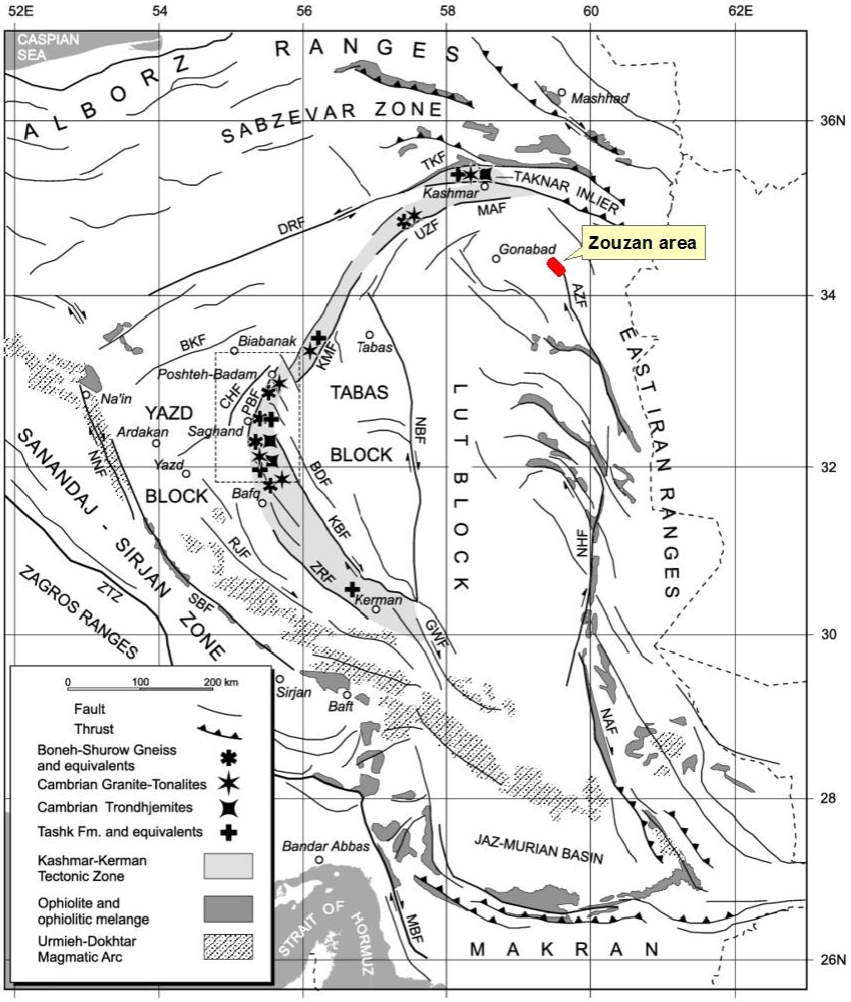

Fig 1. Location of Zouzan Area on Structural map of Central-East Iran compiled based on (Berberian and Berberian 1981; Jackson and McKenzie 1984; Lindenberg et al. 1984; Haghipour 1989; Alavi 1991)

The volcanic rocks include dacitic to rhyodacitic and andesitic lavas that are extensively altered in the vicinity of the younger intrusive rock. The sub volcanic intrusive rocks, the most dominant in the region, consist of five compositional groups, the relative ages of which can be established based on crosscutting relationships and alteration type as follows: 1) hornblende quartz monzonite; 2) biotite-hornblende quartz monzodiorite to monzonite porphyry; 3) hornblende monzonite to monzodiorite porphyry; 4) monzonite porphyry; and 5) hornblende diorite porphyry (Fig 2). The ~ 39 Ma U-Pb radiometric ages obtained from zircon from the host monzonite-diorite porphyries indicate a Middle Eocene age (Shafaroudi et al. 2015). The following alterations observed in Zouzan area can be devided in to 12 zones: carbonate zone, intense propylitic zone, moderate propylitic zone, incipient propylitic zone, sericite - propylitic zone, argillic- propylitic zone, quartz-carbonate zone, Poor sericite zone, quartz-sersite zone, poor silica zone, silica zone, and silica-propylithic zone. In the central parts of the study area, there is some limited skarn parts in contact between the limestones and intrusive bodies, which are poorly mineralized. The mineralization in the sulfide zone has pyrite, chalcopyrite, and galena, which occurs in veins and veinlets, along with silica and argillic alterations. In some areas, this mineralization is accompanied by magnetite, as well as silica veins which occur in the contact of the intrusive bodies and dikes with metamorphic rocks such as schists (Ehsan et al. 2013).

3. Methodology

For geochemical studies, 488 stream sediment samples that were collected by the Geological Survey of Iran (Mashhad branch) in 1998 and chemical analyzed by ICP-MS were used (Azmi 2007).First, statistical parameters were calculated. Statistical results show that Au, Ag, Cu, Pb and Zn average values are 0.003, 0.008, 22.68, 34.78, 87.75ppm, respectively (Table 1). Their distributions are shown in Fig 3 and do not display a normal character. Variation between maximum and minimum for these data shows a wide range. (Afzal et al. 2010). Histogram for each element was plotted (Fig 3). The data were analyzed using multi-stage factor analysis and fractal modeling.

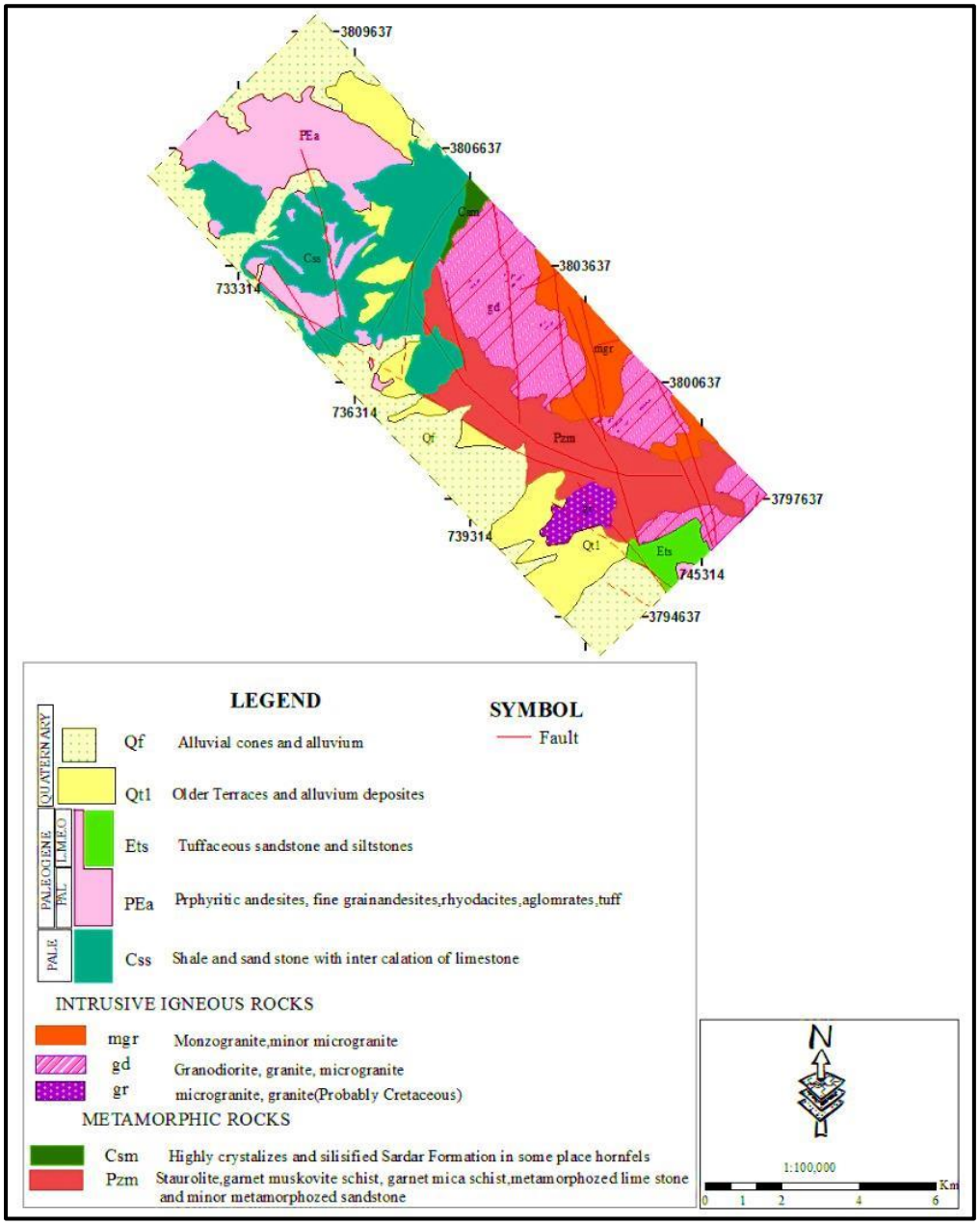

Fig 2.Geology map of Zouzan area (after Blourian and Safari 2005).

Table1. Statistical parameters of the main elements in the Zouzan area

	Au(ppm)	Ag(ppm)	Cu(ppm)	Pb(ppm)	Zn(ppm)
Average	0.003	0.08	22.68	34.78	85.75
Standard Division	0.002	0.08	7.64	37.26	46.91
Max	0.01	0.48	59.4	220	316
Min	0.001	0.01	5.8	11.8	40
Median	0.003	0.06	21.35	21.45	70

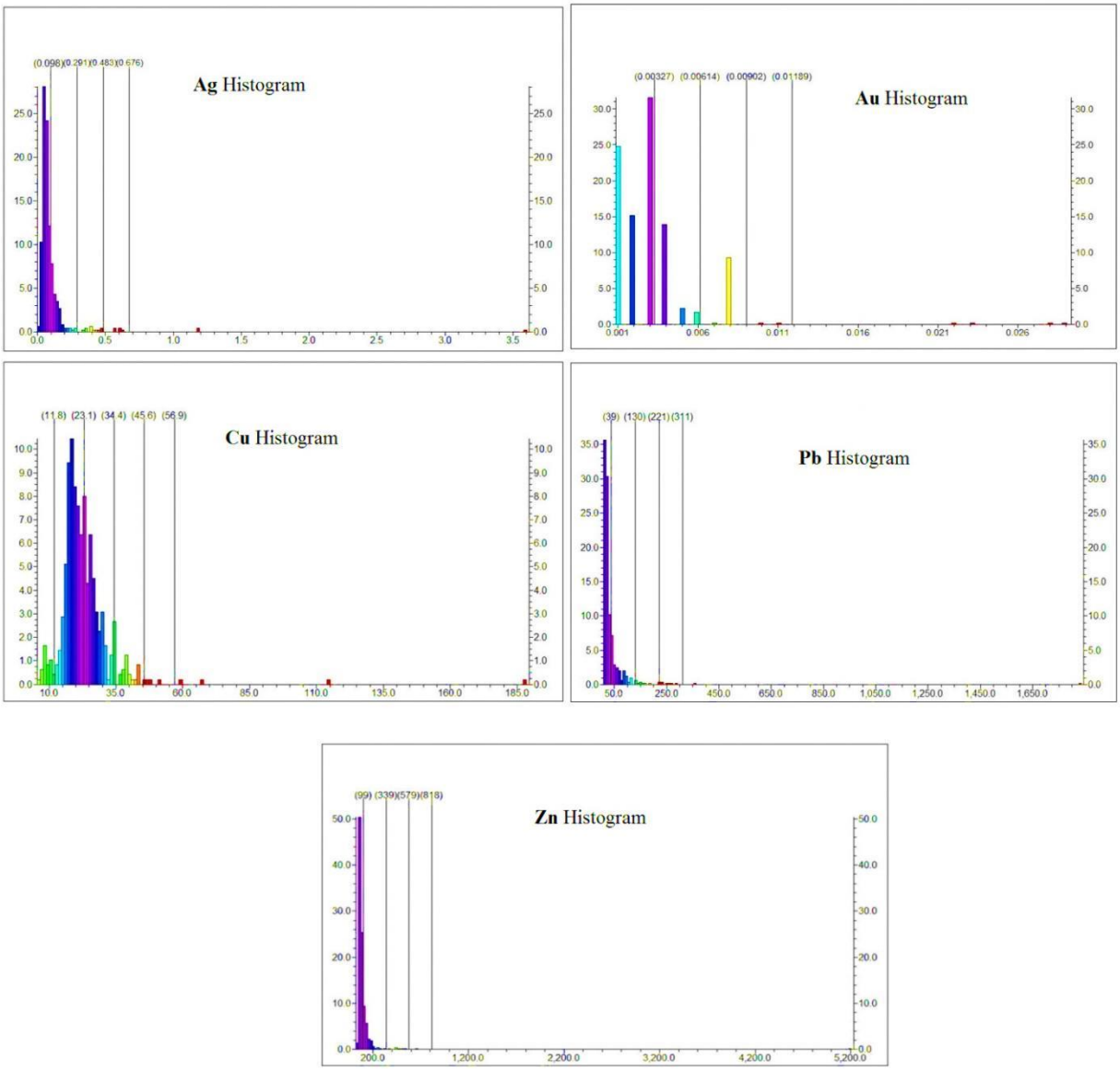

Fig 3.Histogram of the main elements in the Zouzan area

3.1. C-N multi-fractal model

The Number–Size (N–S) fractal model, which was originally proposed (Kirkby 1983), can be used to describe the distribution of geochemical populations without pre-processing of data. Based on that model, the C–N fractal model was proposed (Hassanpour and Afzal 2013) for analyzing the raw data of geological models. This model displays relations between geological attributes (e.g., ore elements in this paper) and their cumulative frequency of samples. The model is expressed by the following formula (Kirkby 1983; Deng et al. 2010; Sadeghi et al. 2012):

$$N (\geq \rho) = F\rho^{-D} \quad (1)$$

where ρ indicates element concentration, N (≥ρ) denotes cumulative number of samples with concentration values greater than or equal to ρ, F is a constant, and D is the scaling exponent or fractal dimension of the distribution of element concentrations. According to (Kirkby 1983) and (Deng et al. 2010), log-log plots of N (≥ρ) versus ρ show straight line segments with different slopes −D corresponding to different concentration intervals. This method is based on the fact that the number of samples is reduced as their concentration increase (Rahmati et al. 2015; Adib et al. 2017; Afzal et al. 2017b; Nabilou et al. 2018; Nazarpour 2018).

3.2. Staged factor analysis

The staged factor analysis proposed by (Yousefi et al. 2012) is based upon the lr- and ilr-transformation that has been developed based on the principal component analysis (PCA) for extraction of factor varimax rotation of factors but it is a multi-step factor analysis to extract

the components showing anomalies in multi-element ore deposit-type-based mineralized stages and ore elements. The use of staged Factor analysis enhances recognition of anomalous geochemical signatures, increases geochemical anomaly intensity, and increases the percentage of the total explained variability of data (Ghadimi et al. 2016; Afzal et al. 2017a; Aliyari et al. 2017).

4. Application of staged factor analysis

The principal component analysis (PCA) was utilized for extraction of factors based on the 14 elemental grade data, and also the varimax rotation of factors was applied using the SPSS software. Second-step factor analysis was used to extract the components illustrating the anomalous multi-element geochemical signatures of the deposit-type sough in the first step, the factor analysis yielded 10 rotated components, each with eigenvalues greater than 0.6 (Table 2). In the second step, some elements were removed, which were not in the any factor, and consisted of Ba, Co, Mn and Sr and the factor analysis was carried out on the other elements. In this step, four factors were determined with the following groups, as depicted in Table 3.

Table 2. Results of the first Stage of staged factor analysis and components that removed

	1	2	3	4	5
Au	-0.002	-0.053	-0.052	-0.013	0.941
Ag	0.932	-0.02	0.05	0.15	-0.005
Ba	-0.016	0.167	-0.722	-0.001	0.123
Cu	0.449	-0.208	0.095	0.813	0.031
Co	0.174	-0.729	0.251	0.305	0.184
Cr	0.102	0.653	0.623	0.105	0.119
Li	0.079	0.227	0.683	0.002	0.06
Mg	-0.001	0.179	0.763	-0.1	0.144
Mn	0.068	-0.843	-0.085	0.203	0.155
Mo	0.031	0.021	-0.078	0.957	-0.035
Pb	0.97	-0.013	0.058	0.126	0.016
Sr	-0.017	0.119	-0.568	-0.056	0.125
Ti	0.068	0.787	0.078	0.181	0.166
Zn	0.981	-0.017	0.02	0.046	0

Table 3. Results of the second Stage of staged factor analysis and final components

	1	2	3	4
Au	0.013	0.001	-0.004	0.986
Ag	0.93	0.054	0.161	-9.261
Cu	0.464	0.007	0.812	-0.002
Cr	0.061	0.937	0.052	-0.017
Li	0.09	0.666	-0.041	-0.042
Mg	0.011	0.759	-0.162	-0.083
Mo	0.021	-0.017	0.973	0.004
Pb	0.966	0.075	0.132	0.007
Ti	-0.017	0.62	0.145	0.155
Zn	0.979	0.03	0.06	0.008

5. Application of C-N multi-fractal model

Raw data was used for the C–N fractal modeling, and the relation between concentration and number was shown in a log-log plot. Considering that abrupt changes in the slopes of conformed straight line segments fitted to the log-log plot represent boundaries between mineralized zones (Rahmati et al. 2015) Fig 4). Elemental populations for Au, Ag, Cu, Pb and Zn were separated by fractal modeling. Log-log plot for Au represented five populations in which the first population includes samples with less than 27 ppb thus defining the background for Au.

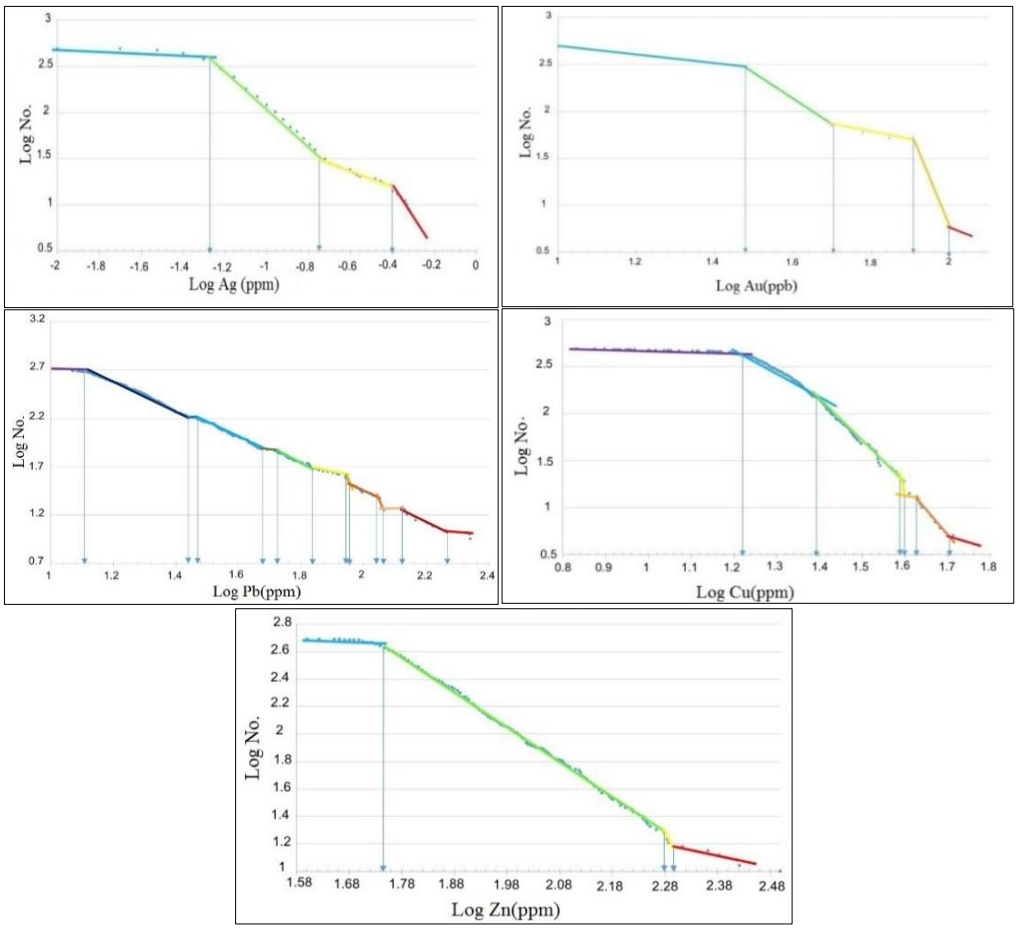

Fig.4. The elemental C-N log-log plots in the Zouzan area

The second population includes samples between 27 ppb to 44 ppb which are the first anomaly of Au. Third population includes samples between 44 ppb to 70 ppb, the fourth population has concentrations between 70 ppb and 100 ppb and finally the last anomaly population for Au has concentrations greater than 100 ppb; these concentrations are high anomalies of Au and are enhanced in the west center and southeast of the study area.

C-N fractal modeling for Ag detected four populations in which the first population has concentrations less than 0.05 ppm representing the background for Ag. The second population has concentrations between 0.05ppm to 0.1 ppm which are the first anomaly of Ag. The third population has concentrations between 0.01ppm to 0.4 ppm and the last anomaly population for Ag has concentrations greater than 0.4 ppm; these concentrations are high anomalies of Ag and are enhanced in the southern, SW and central parts of the study area.

For Cu the C-N model detected seven populations. The first population has concentrations less than 16 ppm representing the background for Cu. The second population has concentrations between 16 ppm to 25 ppm , the third population has concentrations between 25ppm to 39 ppm, concentrations between 39 ppm to 42 ppm in the fourth population for Cu , concentrations between 42 ppm to 50 ppm for the fifth anomaly population for Cu , concentrations between 50 ppm to 60 ppm for the sixth population and the last anomaly population has concentrations greater than 60 ppm; these concentrations are high anomalies of Cu and are enhanced in southwest, center and north parts of the study area. Pb anomalies are distributed in wide area and the C-N modeling shows the sharp anomaly points of that the background concentrations of Pb are less than13 ppm the first anomaly population has concentrations between 13 ppm to 50 ppm the second population of Pb has concentrations between 50 ppm to 90 ppm The third population has concentrations between 90 ppm to 130 ppm the forth population has concentrations between 130ppm to 190ppm and the last anomaly has concentrations greater than 190ppm this population is high concentration for Pb which are enhanced in a NW-SE trend in study area. Finally, for Zn the fractal model has been shown four populations in which the first population has concentrations less than 57 ppm the second population has concentrations

between 57 ppm to 190 ppm which is the first anomaly of Zn third population has concentrations between 190 ppm to 200 ppm the last population has concentrations greater than 200 ppm which are high has concentrations of Zn anomaly and enhanced in southwest, center and north parts of the study area (Fig 5) these concentrations are shown in table 4.

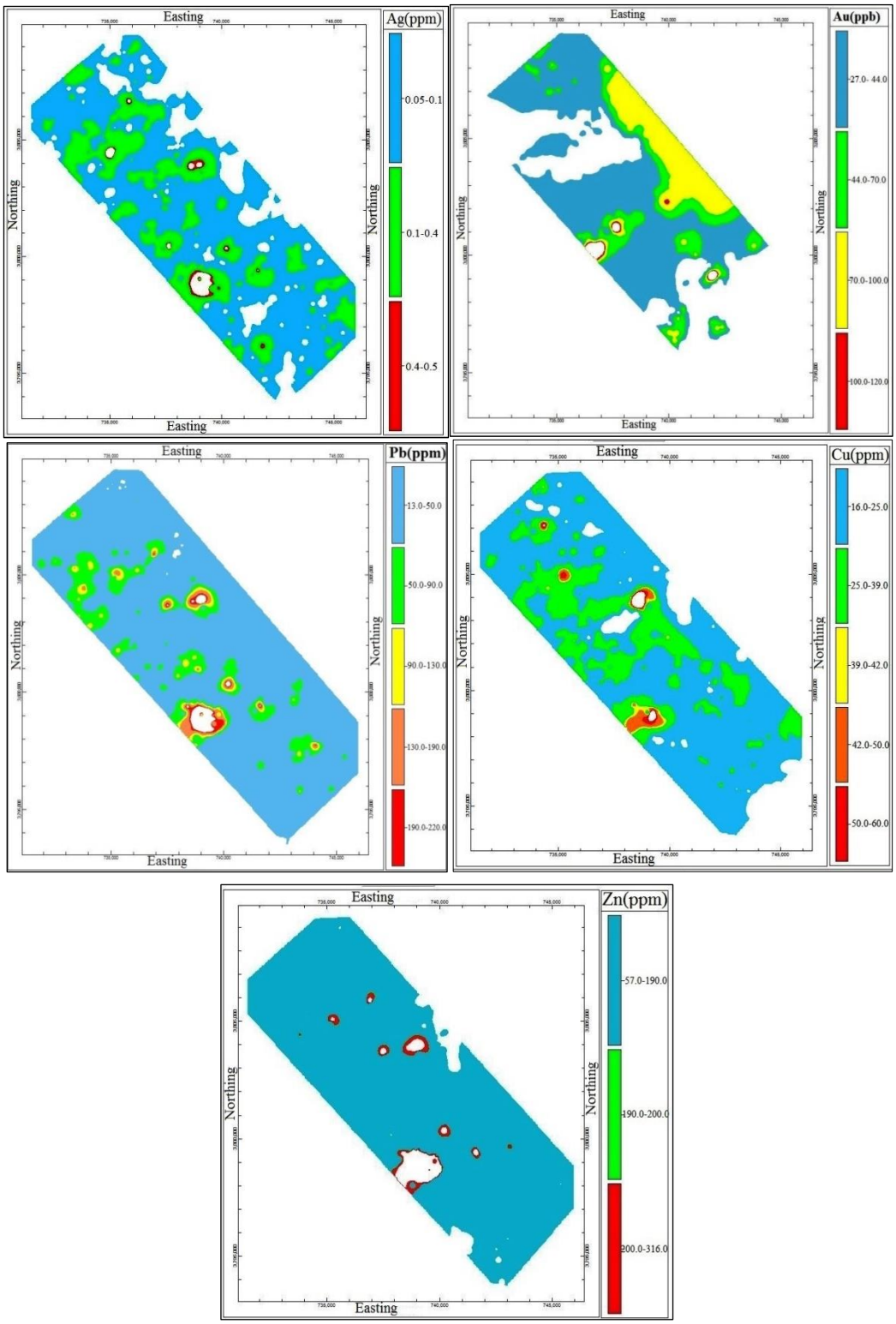

Fig 5. The C-N models of the main elements in the Zouzan area

Fractal modeling was also applied to the data obtained from staged factor analysis and the log-log plots of the components were drawn (Fig 6). It showed in which parts of study Area the components of the parallel elements have enrichment. Based on the fractal model for the four specified factors, the first component includes the Ag, Pb and Zn shows its own enrichment in south west, Centre and north east of the study area; the second component include the Cr, Mn, Li and Ti shows low concentrations in the southern and SE parts of the study area indicating that the enrichment of these elements in the study area isn't in much significant and they can't be effective in this area. The third component include Cu and Mo which is one of the important components in this area shows its own enrichment in the east part of the study area and finally the forth component include Au and enhanced in south, west and center of the study area. This model shows that Au enrichment occurs individually and it does not have any significant correlation with other elements in the Zouzan prospect (Fig 7). Correlation graphs confirm the fractal model associated with the data obtained from the stage factor analysis (Fig 8).

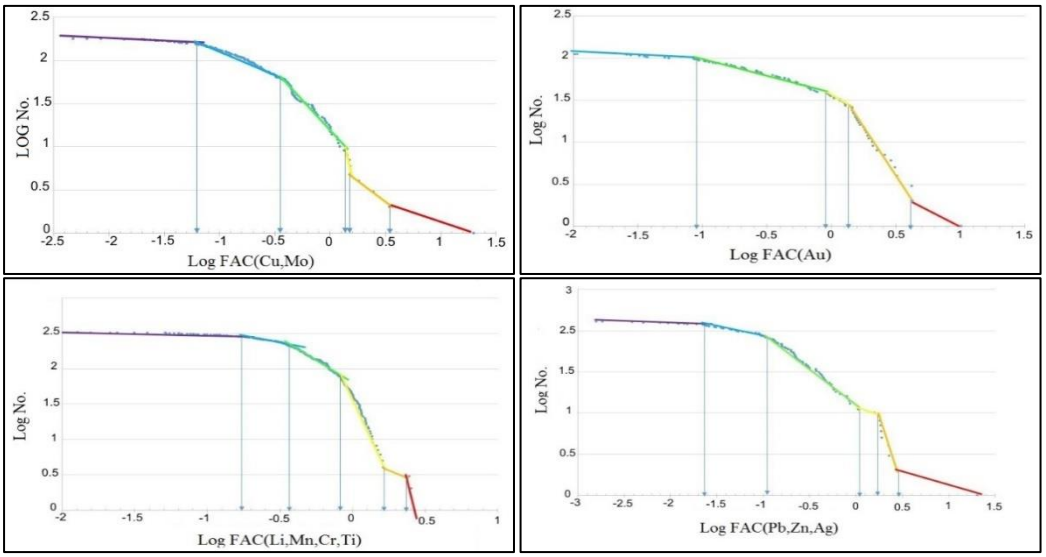

Fi g .6. The C-N log-log plots of the main components obtained by the staged factor analysis in Zouzan prospect

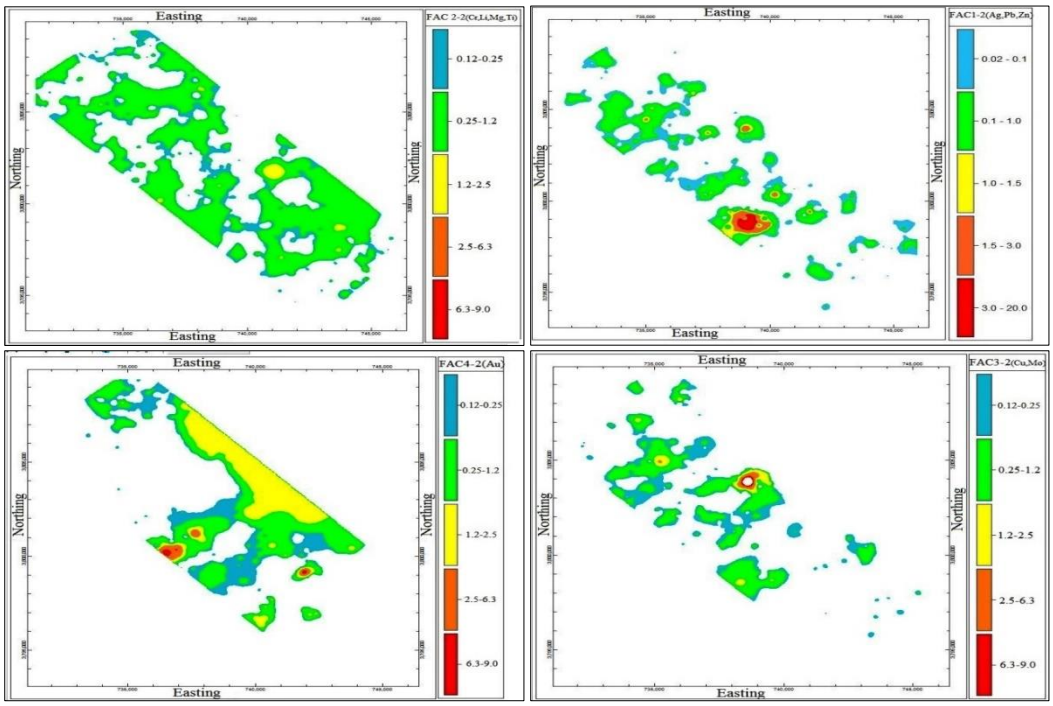

Fig 7. The geochemical maps of the main components obtained by the staged factor analysis in the Zouzan area

Table 4. The main anomaly population of Zouzan area detected by C-N fractal model.

Element / Population	1st	2nd	3rd	4th	5th	6th	7th
Au(ppb)	<27	27 - 44	44-70	70-100	100-120	120<	-
Ag(ppm)	<0.05	0.05-0.1	0.1-0.4	0.4-0.5	0.5<	-	-
Cu(ppm)	<16	16-25	25-39	39-42	42-50	50-60	60<
Pb(ppm)	<13	13-50	50-90	90-130	130-190	190-220	220<
Zn(ppm)	<57	57-190	190-200	200-316	316<	-	-

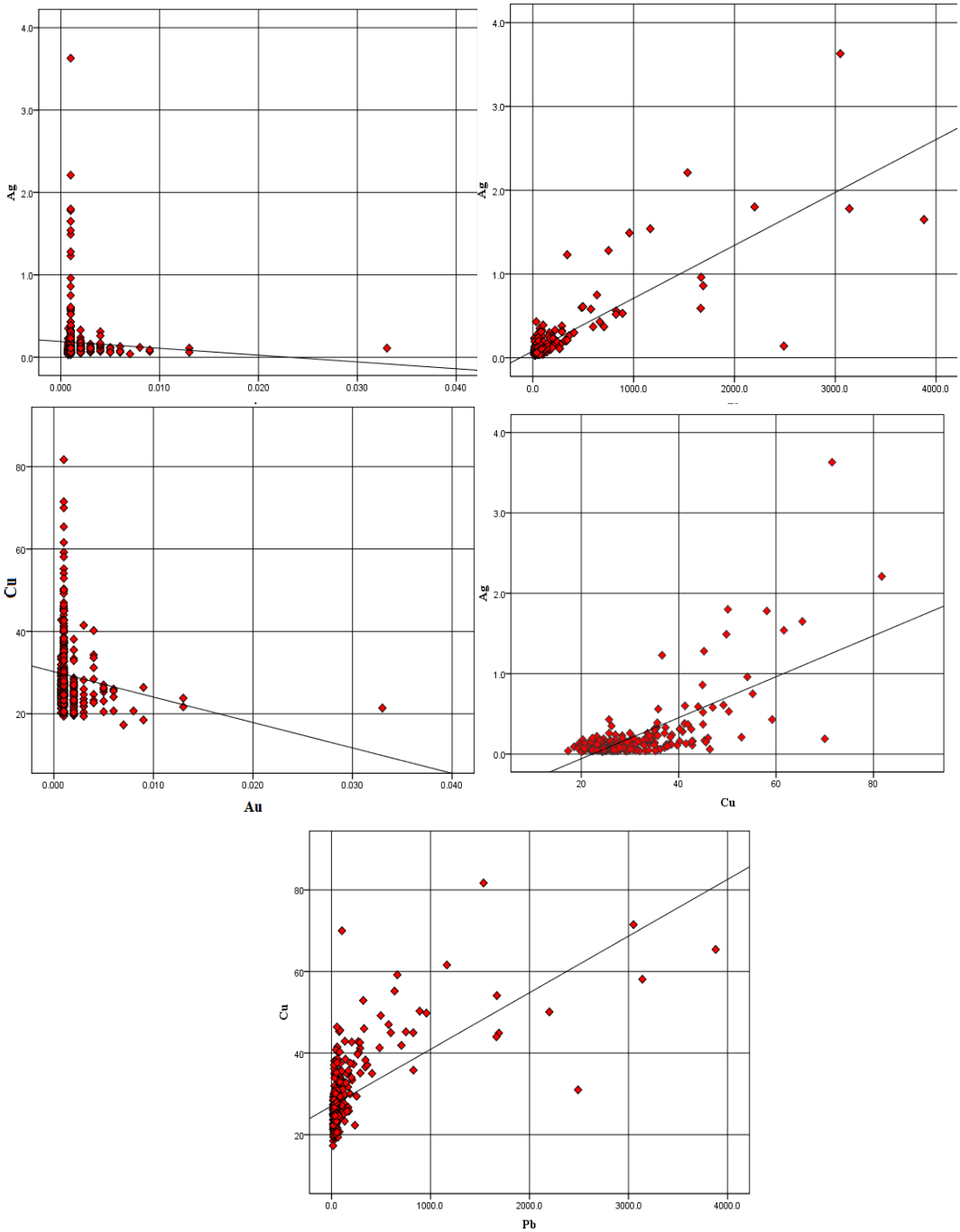

Fig 8. The scatter diagram between the elements in the study area

6. Conclusion

The results obtained by this study show that the CN fractal model is a proper method for separation of different anomalies from background. The classical statistics methods are able to separate only two geochemical populations by median because elemental distribution in most cases are not normal. This process will reduce the accuracy of such studies so utilizing the fractal models could be useful. Moreover, factor analysis could be helped for reduction of variables and separation of multi-elemental anomalies.In this paper, the C-N fractal modeling and staged factor analysis were utilized to delineate the different Au, Ag, Cu, Pb and Zn mineralization zones in the Zouzan area. The models show that the high concentrations of these elements are clustered in central, south east and south west parts of study area the high grade belong to the Pb and Zn which this indicates that the area is rich in Pb and Zn, the Cu also has a significant grade in study area. The concentrations of Au and Ag indicate a polymetalic mineralization with a significant potential in this area. Due to the association of mineralization with each other, the results of the multi stage factor analysis were used to identify four different components, and the fractal modeling of these components showed in which parts of the study area they are correlated with each other. According to the results the Pb, Zn and Ag each other the Cu with Mo, and the Au alone are enriched in the Zouzan area. Also the extent of the fractal model of the components is less than the extent of the elements fractal model but the high anomaly of components is clearer than the high concentrations of the elements so it shows that the combined elements are richer than single phase, the reason for this can be the various phases of mineralization, which has occurred in this area and caused the diversity of the mineralogy.

Acknowledgment

I would like to express my special thanks of gratitude to deceased Professor Ahmad Khakzad as well as Mr. Hassan Saadati Pars Hoorakhsh Company manager, who gave me an opportunity to do this wonderful project, which also helped me in doing a lot of Research and I came to know about so many new things. We are really thankful to them.

References

Adib A, Afzal P, Ilani SM, Aliyari F (2017) Determination of the relationship between major fault and zinc mineralization using fractal modeling in the Behabad fault zone, central Iran, *Journal of African Earth Sciences* 134:308-319.

Afzal P, Heidari SM, Ghaderi M, Yasrebi AB (2017a) Determination of mineralization stages using correlation between geochemical fractal modeling and geological data in Arabshah sedimentary rock-hosted epithermal gold deposit, NW Iran, *Ore Geology Reviews* 91:278-295.

Afzal P, Khakzad A, Moarefvand P, Rashidnejad-Omran N, Esfandiari B, Alghalandis YF (2010) Geochemical anomaly separation by multifractal modeling in Kahang (Gor Gor) porphyry system, Central Iran, *Journal of Geochemical Exploration* 104:34-46.

Afzal P, Yasrebi AB, Saein LD, Panahi S (2017b) Prospecting of Ni mineralization based on geochemical exploration in Iran, *Journal of Geochemical Exploration* 181:294-304.

Alavi M (1991) Tectonic Map of the Middle East, Scale 1:5000000. Tehran: Geological Survey of Iran.

Aliyari F, Afzal P, Abdollahi Sharif J (2017) Determination of geochemical anomalies and gold mineralized stages based on litho-geochemical data for Zarshuran Carlin-like gold deposit (NW Iran) utilizing multi-fractal modeling and stepwise factor analysis, *Journal of Mining and Environment* 8:593-610.

Arjmandzadeh R (2011) Mineralization, geochemistry, geochronology, and determination of tectonomagmatic setting of intrusive rocks in Dehsalm and Chahshaljami prospect areas, Lut block, East of Iran, Unpublished Ph.D thesis, Ferdowsi University of Mashhad, 369pp, (In Persian).

Azmi H (2007) Exploration in Zouzan area using Geochemeical methods in Zouzan area, Exploratory Report of Kan Iran Co, (In Persian).

Berberian F, Berberian M (1981) Tectono-plutonic episodes in Iran, Zagros Hindu Kush Himalaya *Geodynamic Evolution* 3:5-32.

Berberian M (1983) Structural Evolution of the Iranian Plateau; Contribution to the Seismotectonics of Iran, Part IV: Continental Deformation in the Iranian Plateau. Geological Survey of Iran, *Report* 52, 19-68.

Blourian G, Safari M (2005) Geological map of Zouzan, *Geological Survey of Iran*, Tehran, Scale 1: 100,000 (In Persian).

Camp V, Griffis R (1982) Character, genesis and tectonic setting of igneous rocks in the Sistan suture zone, eastern Iran, *Lithos* 15:221-239.

Deng J, Wang Q, Yang L, Wang Y, Gong Q, Liu H (2010) Delineation and explanation of geochemical anomalies using fractal models in the Heqing area, Yunnan Province, China, *Journal of Geochemical Exploration* 105:95-105.

Eftekharnejad J (1981) Tectonic division of Iran with respect to sedimentary basins, *Journal of Iranian Petroleum Society* 82:19-28.

Ehsan S, Hassan KM, Azadeh MS, Shahri H, Reza M (2013) Mineralization, Alteration and Geochemical exploration in the Eastern part of Keybarkuh (Khaf), Unpublished Ph.D thesis, Ferdowsi University of Mashhad, (In Persian).

Ghadimi F, Ghomi M, Aref Sedigh M (2016) Identification of Ti-anomaly in stream sediment geochemistry using of stepwise factor analysis and multifractal model in Delijan district, Iran,

International Journal of Mining and Geo-Engineering 50:77-95.

Golonka J (2004) Plate tectonic evolution of the southern margin of Eurasia in the Mesozoic and Cenozoic, *Tectonophysics* 381:235-273.

Haghipour A, Agha Nabati, A (1989) Geological Map of Iran, *Geological Survey of Iran*, Tehran. Scale 1:2500000 (In Persian).

Hassanpour S, Afzal P (2013) Application of concentration–number (C–N) multifractal modeling for geochemical anomaly separation in Haftcheshmeh porphyry system, NW Iran, *Arabian Journal of Geosciences* 6:957-970.

Jackson J, McKenzie D (1984) Active tectonics of the Alpine-Himalayan Belt between western Turkey and Pakistan, *Geophysical Journal International* 77:185-264.

Jung D, Keller J, Khorasani R, Marcks C, Baumann A, Horn P (1984) Petrology of the Tertiary magmatic activity in the northern Lut area, east Iran, *Neues Jahrbuch für Geologie und Paläontologie-Abhandlungen* 417-467.

Karimpour M (2011) Review of age, Rb-Sr geochemistry and petrogenesis of Jurassic to Quaternary igneous rocks in Lut Block, Eastern Iran, *Geopersia* 1:19-54.

Kirkby M (1983) The fractal geometry of nature. Benoit B. Mandelbrot. WH Freeman and Co., San Francisco, hardback, *Earth Surface Processes and Landforms* 8:405-406.

Lindenberg H, Görler K, Jacobshagen V, Ibbeken H (1984) Postpaleozoic stratigraphy, structure and orogenetic evolution of the southern Sabzewar zone and the Taknar block (Khorassan, NE Iran), *Neues Jahrbuch für Geologie und Paläontologie-Abhandlungen* 287-326.

Mahmoudi S, Masoudi F, Corfu F, Mehrabi B (2010) Magmatic and metamorphic history of the Deh-Salm metamorphic Complex, Eastern Lut block,(Eastern Iran), from U–Pb geochronology, *International Journal of Earth Sciences* 99:1153-1165.

Malekzadeh A (2009) Geology, mineralization, alteration, geochemistry, microthermometry, isotope studies and determining the mineralization source of Khoopic and Maherabad exploration areas. Ph.D thesis. Ferdowsi university of Mashhad, (In Persian).

Nabilou M, Arian M, Afzal P, Adib A, Kazemi A (2018) Determination of relationship between basement faults and alteration zones in Bafq-Esfordi region, central Iran, *Episodes* 41:143-159.

Nazarpour A (2018) Application of CA fractal model and exploratory data analysis (EDA) to delineate geochemical anomalies in the: Takab 1: 25,000 geochemical sheet, NW Iran, *Iranian Journal of Earth Sciences* 10:173-180.

Rahmati A, Afzal P, Abrishamifar SA, Sadeghi B (2015) Application of concentration–number and concentration–volume fractal models to delineate mineralized zones in the Sheytoor iron deposit, Central Iran, *Arabian Journal of Geosciences* 8:2953-2965.

Saadat S, Stern C (2016) Distribution and geochemical variations among paleogene volcanic rocks from the north-central Lut block, Eastern Iran, *Iranian Journal of Earth Sciences* 8:1-24.

Saccani E, Delavari M, Beccaluva L, Amini S (2010) Petrological and geochemical constraints on the origin of the Nehbandan ophiolitic complex (eastern Iran): Implication for the evolution of the Sistan Ocean, *Lithos* 117:209-228.

Sadeghi B, Moarefvand P, Afzal P, Yasrebi AB, Saein LD (2012) Application of fractal models to outline mineralized zones in the Zaghia iron ore deposit, Central Iran, *Journal of Geochemical Exploration* 122:9-19.

Shafaroudi AM, Karimpour MH, Stern CR (2015) The Khopik porphyry copper prospect, Lut Block, Eastern Iran: geology, alteration and mineralization, fluid inclusion, and oxygen isotope studies, *Ore Geology Reviews* 65:522-544.

Stocklin J, Nabavi M (1973) Tectonic map of Iran, *Geological Survey of Iran*.

Tarkian M, Lotfi M, Baumann A (1983) Tectonic, magmatism and the formation of mineral deposits in the central Lut, east Iran, Ministry of mines and metals, GSI, Geodynamic project (geotraverse) in Iran, Geological Survey of Iran, *Report* 51:357-383.

Tirrul R, Bell I, Griffis R, Camp V (1983) The Sistan suture zone of eastern Iran, *Geological Society of America Bulletin* 94:134-150.

Yousefi M, Kamkar-Rouhani A, Carranza EJM (2012) Geochemical mineralization probability index (GMPI): a new approach to generate enhanced stream sediment geochemical evidential map for increasing probability of success in mineral potential mapping, *Journal of Geochemical Exploration* 115:24-35.